Hybrid Analytical-Spectral Method for the Modeling of Piezoelectrically Induced Waves in Plates

Juan Miguel Vivar Perez

HYBRID ANALYTICAL-SPECTRAL METHOD FOR THE MODELING OF PIEZOELECTRICALLY INDUCED WAVES IN PLATES

Juan Miguel Vivar Perez[1]

[1] *German Aerospace Center (DLR), Institute of Composite Structures and Adaptive Systems, Sportallee 54a, 22335 Hamburg*

juan.vivarperez@dlr.de

ABSTRACT

Conventional numerical methods like the Finite Element Method fail to be efficient to model the propagation of ultrasonic guided waves in real structures. The required fine mesh and the the high number of degrees of freedom when solving the wave propagation problem in the time domain lead to a high computational effort and a need of big memory storage capacity. On the other hand, analytical and semi-analytical methods, which offer fast and accurate results, can be only applied to relatively special geometries. In this contribution the use of an hybrid of analytical and spectral methods to model the propagation of elastic guided waves in plates is studied. Guided wave propagation excited by bonded piezoelectric transducers is simulated with this approach. The piezoelectric transducers are modeled using Spectral methods and the response of the plate is calculated using analytical methods. The mathematical modeling of the transducer-plate interface bonding conditions is presented. These conditions are subsequently discretized using an hybrid analytic-spectral formulation in the frequency domain. The numerical accuracy of the obtained results is verified by comparison with other numerical methods such as the finite element method.

KEYWORDS : *Analytical Methods; Spectral Finite Elements; Piezoelectricity, Structural Health Monitoring, Lamb Waves*

INTRODUCTION

Elastic ultrasonic waves in plates have recently found an application in non-destructive testing and therefore, the effort to model elastic waves in plates has increased. Analytical methods like, the Fourier transform and the Cauchy's theorem of residues has been used in the works of Gomilko et al. [1], Raghavan et al. [2] and Giurgiutiu [3]. Alternatively Wilcox [4] applied the concept of excitation matrix to model Lamb wave fields excited by line and point distribution of forces. The modal analysis has also been considered in order to obtain analytical solutions, as in the work of Jin [5]. Another analytical approach is the use of the Green's tensor for point forces in the surface of the three-dimensional model of the plate. This can be seen in the works of Karmazin et al. [6] and Glushkov et al. [7].

Parallel to the analytical approaches mentioned above, other numerical and semi-analytical approaches have been used to model Lamb waves such as the Local Interaction Simulation Approach [8], the Finite Element Method [9], the Spectral Analysis [10], the Spectral Element Method in the time domain in the [11–13], the Spectral Element Method in the frequency domain with the use of the Fast Fourier or the Wavelet Transform [14, 15] as well as the Semi-Analytic Finite Element Method [16–18]. A nice comparison and overview of different higher order finite element formulations applied to the modeling of Lamb wave propagation can be found in [19]. Some mixed formulations have been applied as well in order to keep advantages and decrease disadvantages of different methods such as by a combination of semi-analytic finite elements and standard finite elements [18] and also by a combination of some analytical methods with finite element solutions [20], to mention just a few.

The evaluation of analytical methods is relatively inexpensive. Furthermore, the qualitative behavior of Lamb wave propagation can be derived from the analytical expressions. They have the disadvantage of being only developed for specific geometries. The direct application of purely numerical methods such as the Finite Element Method is the most commonly used approach due to their flexibility to model arbitrary geometries. However, it is the most expensive method in terms of computational effort, since the number of elements and degrees of freedoms in the model increase when rapid variation of the solution in very small subdomains of the integration domain is expected, as in the case of modeling ultrasonic Lamb waves.

This work proposes the development of hybrid formulations that use an analytic approach in big regions of the plate and apply discrete approximation approaches in small regions where perturbation of the plate-like geometry occurs. Our research focuses on the excitation and reception of waves by piezoelectric actuators and sensors. Our aim was reached using spectral elements in the frequency domain to model any perturbation of the plate geometry instead of the classical Finite Element Method. Spectral analysis has a higher order of accuracy as it has been shown in [21], [22] and [11] among others. Semi-analytical expressions for the propagation of Lamb waves were obtained using the concept of the dynamic reaction or response matrix. With this no discretization through the thickness of the plate has to be used as in the works presented in [23] or [18] just to mention some.

1. BONDED PIEZOELECTRIC TRANSDUCERS

A piezoelectric transducer bonded to an infinite isotropic plate is considered. Piezoelectric actuator has a volume Ω and shares the the interface Γ with the plate as represented in figure figure 1.

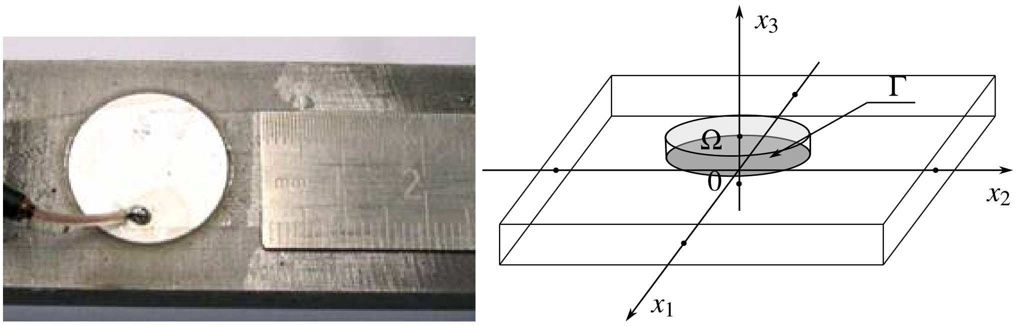

Figure 1 : Piezoelectric patch bonded to a plate (left). The piezoelectric patch occupies a volume Ω and shares a common interface Γ with the plate (right).

We analyze the governing equations of the piezoelectric patch and of the plate separately. The bounding conditions on the interface Γ will be modeled as special boundary conditions. Two separated problems are derived. The first problem corresponds to wave propagation on the plate due to dynamic loads applied on its upper surface, and the other corresponds to the electromechanical behavior of the piezoelectric patch under appropriate boundary conditions in Γ that model the influence of the reaction forces of the plate on the actuator or sensor. A graphical representation of this idea is given in figure 2.

The displacement field in the plate resulting from the applied loads found with analytical methods. The modeling of the behavior of the piezoelectric sensor/actuator is done using high order (spectral) finite elements.

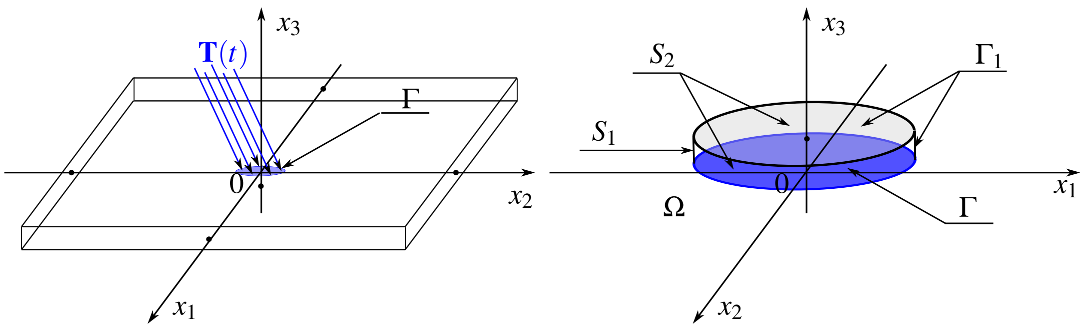

Figure 2 : The dynamic analysis of the plate and the piezoelectric patch is done separately. A plate is considered and the influence of the actuator or sensor is modeled as a dynamic load $\mathbf{T}$ applied to the surface Γ(left). The piezoelectric transducer is considered and the reaction forces of the plate are modeled by special boundary conditions on the surface Γ(right).

2. Analytical methods in isotropic plates

A homogeneous linear elastic isotropic plate of thickness d under a distribution of dynamic loads $\mathbf{T}$ is considered (figure 2). Using the concept of Green's tensor the following integral relation between the Fourier transform of the displacements $\mathbf{u}^*$ and the Fourier transform of the loads $\mathbf{T}^*$ can be established

$$\mathbf{u}^*(\bar{\mathbf{x}}, x_3; \omega) = \int_{\mathbb{R}^2} \mathbf{E}^*(\bar{\mathbf{x}} - \bar{\mathbf{x}}', x_3; \omega) \cdot \mathbf{T}^*(\bar{\mathbf{x}}'; \omega) d\bar{\mathbf{x}}'. \quad (1)$$

The bar over $\mathbf{x}$ denotes that the this position vector depends only on x_1 and x_2 and ω is the circular frequency. The Green's tensor $\mathbf{E}^*$ can be given analytically [6, 20].

$$\mathbf{E}^* = \sum_{n=0}^{\infty} \left\{ \mathbf{E}^A(x_3; \xi_n^A, \omega) e^{i\xi_n^A x} + \mathbf{E}^S(x_3; \xi_n^S, \omega) e^{i\xi_n^S x} + \mathbf{E}^a(x_3; \xi_n^a, \omega) e^{i\xi_n^a x} + \mathbf{E}^s(x_3; \xi_n^s, \omega) e^{i\xi_n^s x} \right\} \quad (2)$$

where x is the vector length of the first argument of $\mathbf{E}^*$ in (1). The matrix functions $\mathbf{E}^A$, $\mathbf{E}^S$, $\mathbf{E}^a$ and $\mathbf{E}^s$ correspond to the antisymmetric Lamb modes, the symmetric Lamb modes, the antisymmetric shear horizontal (SH) modes and the symmetric SH modes, respectively.

$$\mathbf{E}^A(x_3; \xi, \omega) = \frac{i}{2\mu} \begin{pmatrix} \frac{N^A_{\xi\xi}}{\partial D_A/\partial \xi} & 0 & \frac{N^A_{\xi 3}}{\partial D_A/\partial \xi} \\ 0 & 0 & 0 \\ \frac{N^A_{3\xi}}{\partial D_A/\partial \xi} & 0 & \frac{N^A_{33}}{\partial D_A/\partial \xi} \end{pmatrix}, \quad \mathbf{E}^a(x_3; \xi, \omega) = \frac{i(-1)^n}{\mu \xi d} \sin \frac{(2n+1)\pi x_3}{d} \begin{pmatrix} 0 & 0 & 0 \\ 0 & 1 & 0 \\ 0 & 0 & 0 \end{pmatrix},$$
$$\mathbf{E}^S(x_3; \xi, \omega) = \frac{i}{2\mu} \begin{pmatrix} \frac{N^S_{\xi\xi}}{\partial D_S/\partial \xi} & 0 & \frac{N^S_{\xi 3}}{\partial D_S/\partial \xi} \\ 0 & 0 & 0 \\ \frac{N^S_{3\xi}}{\partial D_S/\partial \xi} & 0 & \frac{N^S_{33}}{\partial D_S/\partial \xi} \end{pmatrix}, \quad \mathbf{E}^s(x_3; \xi, \omega)_n = \frac{i(-1)^n}{\kappa_n \mu \xi d} \cos \frac{2n\pi x_3}{d} \begin{pmatrix} 0 & 0 & 0 \\ 0 & 1 & 0 \\ 0 & 0 & 0 \end{pmatrix}. \quad (3)$$

In (3) we apply the convention $\kappa_0 = 2$ and $\kappa_n = 1$ for $n > 0$. The functions N in the numerators are as follows

$$
\begin{aligned}
N^A_{\xi\xi}(x_3;\xi,\omega) &= q\left[2\xi^2 \sin\frac{qd}{2}\sin px_3 - (\xi^2-q^2)\sin\frac{pd}{2}\sin qx_3\right],\\
N^S_{\xi\xi}(x_3;\xi,\omega) &= q\left[-2\xi^2 \cos\frac{qd}{2}\cos px_3 + (\xi^2-q^2)\cos\frac{pd}{2}\cos qx_3\right],\\
N^A_{3\xi}(x_3;\xi,\omega) &= -i\xi\left[2pq \sin\frac{qd}{2}\cos px_3 + (\xi^2-q^2)\sin\frac{pd}{2}\cos qx_3\right],\\
N^S_{3\xi}(x_3;\xi,\omega) &= -i\xi\left[2pq \cos\frac{qd}{2}\sin px_3 + (\xi^2-q^2)\cos\frac{pd}{2}\sin qx_3\right],\\
N^A_{\xi 3}(x_3;\xi,\omega) &= i\xi\left[(\xi^2-q^2)\cos\frac{qd}{2}\sin px_3 + 2pq\cos\frac{pd}{2}\sin qx_3\right],\\
N^S_{\xi 3}(x_3;\xi,\omega) &= i\xi\left[(\xi^2-q^2)\sin\frac{qd}{2}\cos px_3 + 2pq\sin\frac{pd}{2}\cos qx_3\right],\\
N^A_{33}(x_3;\xi,\omega) &= p\left[(\xi^2-q^2)\cos\frac{qd}{2}\cos px_3 - 2\xi^2\cos\frac{pd}{2}\cos qx_3\right],\\
N^S_{33}(x_3;\xi,\omega) &= p\left[-(\xi^2-q^2)\sin\frac{qd}{2}\cos px_3 + 2\xi^2\sin\frac{pd}{2}\cos qx_3\right],
\end{aligned}
\tag{4}
$$

and the functions D have are given by the following expressions

$$
\begin{aligned}
D_A &= 4\xi^2 pq\cos\frac{pd}{2}\sin\frac{qd}{2} + (\xi^2-q^2)^2\sin\frac{pd}{2}\cos\frac{qd}{2},\\
D_S &= 4\xi^2 pq\sin\frac{pd}{2}\cos\frac{qd}{2} + (\xi^2-q^2)^2\cos\frac{pd}{2}\sin\frac{qd}{2},
\end{aligned}
\tag{5}
$$

with,

$$
p^2 = \frac{\omega^2}{c_1^2} - \xi^2 \quad q^2 = \frac{\omega^2}{c_2^2} - \xi^2, \quad c_1^2 = \frac{\lambda+2\mu}{\rho}, \quad c_2^2 = \frac{\mu}{\rho}. \tag{6}
$$

where λ and μ are the first and second Lamé elastic constants and ρ the mass density of the plate. The wavenumbers ξ_n^A and ξ_n^S are frequency dependent and are the solutions of the Rayleigh-Lamb dispersion equations for antisymmetric and symmetric Lamb modes, say $D_A = 0$ and $D_S = 0$respectively. The wavenumbers ξ_n^a and ξ_n^s corresponding to antisymmetric and symmetric SH modes can be given explicitly, as

$$
\xi_n^a = \sqrt{\frac{\omega^2}{c_2^2} - \frac{(2n+1)^2\pi^2}{d^2}}, \quad \xi_n^s = \sqrt{\frac{\omega^2}{c_2^2} - \frac{4n^2\pi^2}{d^2}}. \tag{7}
$$

In figure 3 the dependence between the wavenumbers and the frequency is illustrated. The dispersion

Table 1 : Material data for aluminum

Longitudinal/Trasnversal velocity	**(m/s)**
c_1	6197
c_2	3121

curves of the dependence on the frequency of the wave numbers of the antisymmetric and the symmetric Lamb modes, ξ_n^A and ξ_n^S and ξ_n^a and ξ_n^s of the antisymmetric and the symmetric SH modes can be observed for an aluminum plate. The values of the material constants required for the calculation are given in table 1.

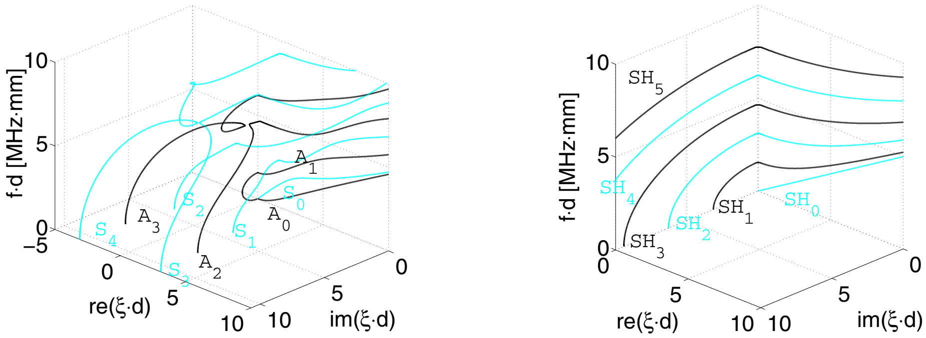

Figure 3 : Graphical representation of the wavenumber-frequency dependence corresponding to the first symmetric and the antisymmetric Lamb (Left) and SH (right) modes in an aluminum plate. Curves corresponding to symmetric and antisymmetric modes are represented in light and dark color, respectively.

3. Spectral analysis for bonded piezoelectric patches

The governing equations in frequency domain of the piezoelectric patch illustrated in figure 2 are as follows

$$\begin{aligned} c_{ijkl}u^*_{k,lj} + e_{lij}\phi^*_{,lj} &= -\omega^2\rho u^*_i \\ e_{jkl}u^*_{k,lj} - \varepsilon_{lj}\phi^*_{,lj} &= 0. \end{aligned} \tag{8}$$

Einstein's summation convention regarding the sum over repeated indexes k, l and j is considered and an index j after a comma denotes a partial derivative with respect to the variable x_j. Here $\mathbf{u}^*$ and ϕ^* are the Fourier transform of the vector of displacements and electric potential, respectively. The tensors $\mathbf{c}$, $\mathbf{e}$ and ε are the elasticity, piezoelectric and dielectric tensors, respectively and ρ is the mass density. The boundary conditions can be stated in the following form

$$\begin{aligned} \left(c_{ijkl}u^*_{k,l} + e_{lij}\phi^*_{,l}\right) n_j\big|_{\Gamma_1} &= 0, \\ \left(e_{jkl}u^*_{k,l} - \varepsilon_{jl}\phi^*_{,l}\right) n_j\big|_{S_1} &= 0, \\ \phi^*|_{S_2} &= \gamma^*. \end{aligned} \tag{9}$$

In the interface Γ none of the boundary condition type given in (9) apply and it is studied separately. Consider the Fourier transform of vector of reaction forces of the plate to the bonding denote it by $\mathbf{Q}^*$. Using (1) we can relate the fields $\mathbf{u}^*$ and $\mathbf{Q}^*$ in Γ

$$\mathbf{u}^*(\bar{\mathbf{x}}, d/2; \omega) = \int_\Gamma \mathbf{E}^*(\bar{\mathbf{x}} - \bar{\mathbf{x}}', d/2; \omega)\mathbf{Q}^*(\bar{\mathbf{x}}'; \omega) d\bar{\mathbf{x}}' \qquad \bar{\mathbf{x}} \in \Gamma. \tag{10}$$

The system of equations in (8) together with the boundary conditions in (9) and (10) complete the formulation of the problem corresponding to the dynamic behavior to a bonded piezoelectric patch. Once the distribution of reaction forces $\mathbf{Q}^*$ is determined the displacements in a any point of the plate can be calculated with (1).

To solve this problem and according to the geometry of the piezoelectric atuator a discretization with spectral elements as in figure 4 of the domain Ω is considered. After this is done, the linear system of equations corresponding to the condition (10) reduces to

$$\mathbb{U}^*_I = \mathbb{E}^*\mathbb{Q}^*. \tag{11}$$

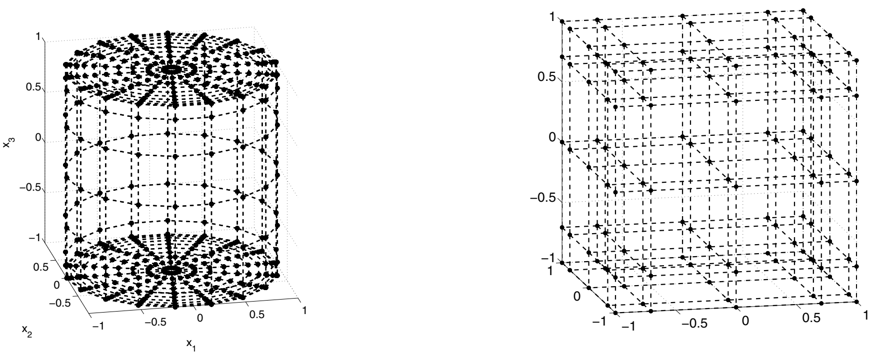

Figure 4 : Different reference spectral (elements) grid models to discretize the two dimensional region Γ and the volume Ω of the bonded piezoelectric actuator.

The components of the vector $\mathbb{U}_I^*$ are the degrees of freedom related to the nodes that belongs to the interface Γ, the receptance matrix $\mathbb{E}^*$ is obtained from the application of the approximated integration in (10) and its entries represent a measure of the plate receptance to the loads $\mathbb{Q}^*$ in Γ induced by the piezoelectric patch. The entry in the *m*-th row and the *n*-th column can be interpreted as the response in the degree of freedom *m* due to a unit force considered in the *n*-th entry of the vector $\mathbb{Q}^*$.

If $\mathbb{K}$ and $\mathbb{M}$ are the stiffness and mass matrices of this system then the dynamic stifness matrix can calculated as $\mathbb{K}^* = \mathbb{K} + \omega^2\mathbb{M}$ and the final system of linar equation for the bonded piezoelectric actuator takes the form

$$\begin{pmatrix} \mathbb{K}_{BB}^* & \mathbb{K}_{BI}^* \\ \mathbb{K}_{IB}^* & \mathbb{K}_{II}^* + (\mathbb{E}^*)^{-1} \end{pmatrix} \begin{pmatrix} \mathbb{U}_B^* \\ \mathbb{U}_I^* \end{pmatrix} = \begin{pmatrix} \mathbb{F}_B^* \\ \mathbb{F}_I^* \end{pmatrix}. \tag{12}$$

The subscript *B* stand for the degrees of freedom related to nodes in the body of the patch that not belong to Γ. The vector $\mathbb{Q}^*$ is determined through the following formula

$$\mathbb{Q}^* = \left\{ \left[\mathbb{K}_{II}^* - \mathbb{K}_{IB}^* (\mathbb{K}_{BB}^*)^{-1} \mathbb{K}_{BI}^* \right] \mathbb{E}^* + \mathbb{I} \right\}^{-1} \left\{ \mathbb{F}_I^* - \mathbb{K}_{IB}^* (\mathbb{K}_{BB}^*)^{-1} \mathbb{F}_B^* \right\}, \tag{13}$$

where $\mathbb{I}$ is the identity matrix of the same size as $\mathbb{E}^*$.

4. NUMERICAL RESULTS AND COMPARISON

In order to verify the reliability of the methods. We consider a 2D-Model of a PIC-181 piezoelectric transducer perfectly bonded to an aluminum plate as shown in figure 5. In our model $d = 2$mm, $a = 1$mm and $b = 10$mm the potential applied on the upper face of the piezoelectric actuator varies according to a 3-cycle modulated sinus with a frequency of 200KHz and amplitude of 50V (figure 5, right side). The displacements at some point of the plate were calculated also with a Finite-Element-Model. The results of the comparison for a point located at $x_1 = 245$mm in the top surface of the plate can be seen in figure 6.

CONCLUSION

A hybrid Analytical-Spectral Method has been developed for the Modeling of ultrasonic waves in plates generated by piezoelectric transducers. The reliability of the method to model the behavior of wave propagation in plates is shown. It offers a significant savings in computational cost when modeling ultrasonic guided waves.

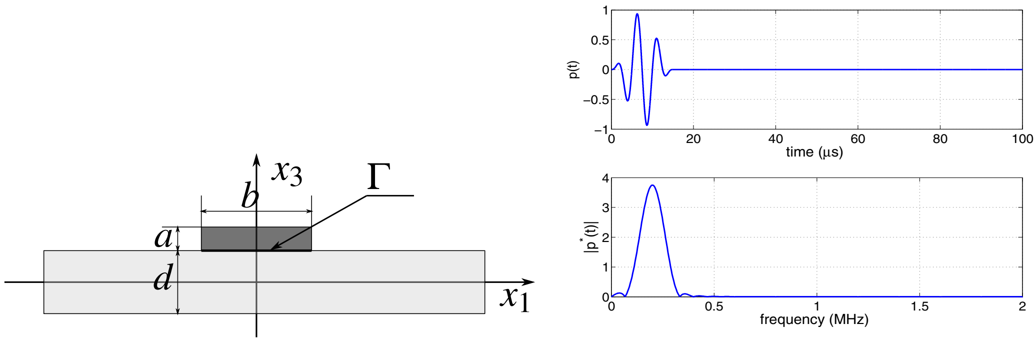

Figure 5 : Geometrical representation of the two-dimensional model for numerical comparison (left) and modulating function $p(t)$ and the absolute value of its Fourier trasform $|p^*(f)|$(right).

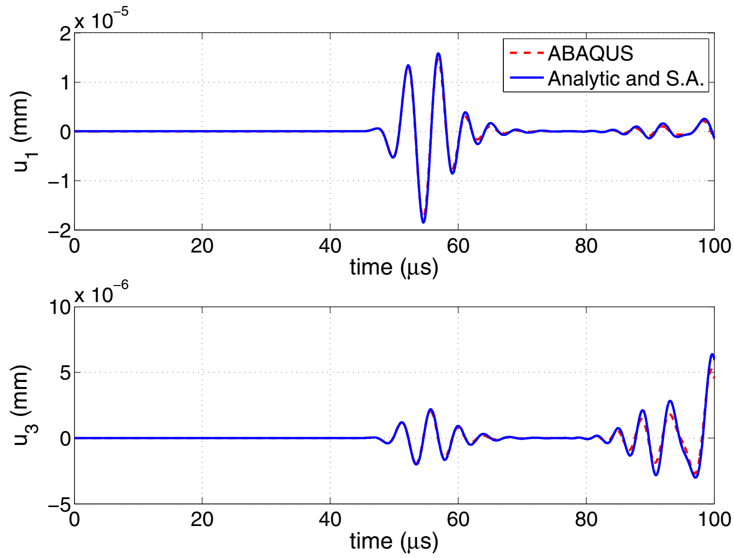

Figure 6 : Vertical and horizontal displacements at point $x_1 = 245$mm on the surface of the plate excited by a piezoelectric actuator. The ABAQUS results are compared with the proposed method (combination of analytical and spectral methods).

REFERENCES

[1] A. M. Gomilko and N. S. Gorodetskaya und V. V. Meleshko. Longitudinal lamb waves in a semi-infinite elastic layer. *International Applied Mechanics*, 27(6):577–581, 1991.

[2] Ajay Raghavan and Carlos E. S. Cesnik. Modeling of piezoelectric-based lamb wave generation and sensing for structural health monitoring. *Proceedings SPIE*, 5391:419–430, 2004.

[3] Victor Giurgiutiu. Tuned Lamb wave excitation and detection with piezoelectric wafer active sensors for structural health monitoring. *Journal of Intelligent Material Systems and Structures*, 16:291–305, 2005.

[4] P. Wilcox. Modeling the excitation of Lamb and SH waves by point and line sources. *AIP Conference Proceedings*, 700:206–213, July 2004.

[5] J. Jin, S. T. Quek, and Q. Wang. Analytical solution of excitation of lamb waves in plates by inter-digital transducers. *Proceedings of the Royal Society A*, 459:1117–1134, 2003.

[6] Alexander Karmazin, Evgenia Kirillova, Wolfgang Seemann, and Pavel Syromyatnikov. Investigation of lamb elastic waves in anisotropic multilayered composites applying the green's matrix. *Ultrasonics*, 51(1):17–28, 2011.

[7] Ye.V. Glushkov, N.V. Glushkova, and A.S. Krivonos. The excitation and propagation of elastic waves in multilayered anisotropic composites. *Journal of Applied Mathematics and Mechanics*, 74(3):297–305, 2010.

[8] P.P. Delsanto, R.S. Schechter, and R.B. Mignogna. Connection machine simulation of ultrasonic wave propagation in materials iii: The three-dimensional case. *Wave Motion*, 26(4):329–339, 1997.

[9] Baiqiang Xu, Zhonghua Shen, Xiaowu Ni, , and Jian Lu. Numerical simulation of laser-generated ultrasound by the finite element method. *Journal of Applied Physics*, 95(4):2116– 2121, 2004.

[10] J. M. Vivar-Perez, C. Willberg, and U. Gabbert. Simulation of piezoelectric Lamb waves in plate structures. In *International Conference on Structural Engineering Dynamics. ICEDyn Ericeira, Portugal. 22.-24. Juni*, 2009.

[11] Wieslaw Ostachowicz, Pawel Kudela, Marek Krawczuk, and Arkadiusz Zak. *Guided Waves in Structures for SHM: The Time-Domain Spectral Element Method*. John Wiley & Sons, Ltd, 2012.

[12] P. Kudela and W. M. Ostachowicz. 3D time-domain spectral elements for stress waves modelling. *Journal of Physics*, 181(1):1–8, 2009.

[13] Haikuo Peng, Guang Meng, and Fucai Li. Modeling of wave propagation in plate structures using three-dimensional spectral element method for damage detection. *Journal of Sound and Vibration*, 320:942–954, 2009.

[14] S. Gopalakrishnan, A. Chakraborty, and D. Roy Mahapatra. Spectral finite element method. In Klaus-Jrgen Bathe, editor, *Computational Fluid and Solid Mechanics*, volume XIV. Springer, 2008.

[15] Gopalakrishnan S., S. Gopalakrishnan, and M. Mitra. *Wavelet Methods for Dynamical Problems: With Application to Metallic, Composite, and Nano-Composite Structures*. Crc Pr Inc, 2010.

[16] J. M. Galn and R. Abascal. Numerical simulation of lamb wave scattering in semi-infinite plates. *International Journal for Numerical Methods in Engineering*, 53(5):1145–1173, 2002.

[17] Ivan Bartoli, Alessandro Marzania, Francesco Lanza di Scalea, and Erasmo Violab. Modeling wave propagation in damped waveguides of arbitrary cross-section. *Journal of Sound and Vibration*, 295(3-5):685–707, 2006.

[18] Z. A. B. Ahmad. Numerical simulations of waves in plates using a semi-analytical finite element method. In *Fortschritt-Berichte VDI*, number 437 in Reihe 20-Rechnerunterstttze Verfahren. VDI Verlag, 2011.

[19] C. Willberg, S. Duczek, J. M. Vivar-Perez, D. Schmicker, and U. Gabbert. Comparison of different higher order finite element schemes for the simulation of lamb waves. *Computer Methods in Applied Mechanics and Engineering*, 241-244:246–261, 2012.

[20] J. M. Vivar-Perez. *Analytical and Spectral methods for the Simualtion of Elastic Waves in Thin Plates*. Number 441 in Reihe 20. Fortschrit-Berichte VDI. VD, 2012.

[21] John P. Boyd. *Chebyshev and Fourier Spectral Methods*. Dover, 2. edition edition, 2000.

[22] Lloyd M. Trefethen. *Spectral Methods in MATLAB*. SIAM, 2000.

[23] P. W. Loveday. Analysis of piezoelectric ultrasonic transducers attached to waveguides using waveguide finite elements. *IEEE transactions on ultrasonics, ferroelectrics, and frequency control*, 54(10):2045–2051, October 2007.